A novel hybrid self-assembly process for synthesising stratified polyethylene-organoclay films

Ali Akbar Motedayen, Carole Guillaume, Emmanuelle Gastaldi, Olivier Felix, Nathalie Gontard

A novel hybrid self-assembly process for synthesising stratified polyethylene–organoclay films

Ali Akbar Motedayen,[a] Carole Guillaume,[b] Emmanuelle Gastaldi,[b] Olivier Félix[c] and Nathalie Gontard[*,a]

[a] UMR IATE, INRA, 2 Place Pierre Viala, F-34060 Montpellier Cedex 1, France.
[b] UMR IATE, University of Montpellier, 2 Place Eug`ene Bataillon, 34090 Montpellier Cedex 1, France
[c] Institut Charles Sadron (CNRS-ULP), 23 rue du Loess, 67034 Strasbourg Cedex 2, France

Corresponding author: E-mail: gontard@univ-montp2.fr; Tel: +33 612231467

Abstract
This study reports the first effort to synthesize a new type of PE–organoclay multilayer film by starting from an uncharged apolar polymer substrate and successively depositing apolar organoclay and uncharged apolar polyethylene (PE) layers with subsequent repeating depositions. The alternate variation of contact angle (85° average for organoclay and 107° for PE layers) confirmed the profilometry and the scanning electron microscopy results as well as the linear growth pattern, *i.e.* the successful highly stratified assembly of repetitive bilayers comprised of 450 nm organoclays and 2.25 µm PE layers. The selfassembly of organoclays on PE surfaces was driven by solvophobic molecular construction involving hydrophobic interactions between the organic parts of the organoclay tactoids dispersed in an organic solvent and the PE hydrophobic surface. The deposition of PE molecules on the organoclay layers was the result of a dip-coating process involving physical sorption of a highly viscous PE solution on the surface of the organoclay layers.

Introduction
The attractive properties and potential usages of nano-enabled composite materials are growing extensively.[1] Combining nanoparticles (NPs) with compatible polymers, aims to design composites with enhanced functional properties such as improved mechanical strength,[2] enhanced thermal stability,[3] increased electrical conductivity,[4] enhanced flame retardancy[5] and/or improved barrier properties.[6] In the extensive field of nano-materials, food packaging, which primarily aims to facilitate food preservation and safety, is one of the most promising and advanced areas in terms of R&D and commercial applications.[7] A wide variety of NPs (organic/mineral nano-spheres, -tubes or -clays) is the key aspect in the development of innovative packaging materials. Many reviews present the latest advances in elaboration strategies of nano-enabled composites and the resulting functional properties, mainly mechanical[1,8,9] and barrier properties,[10–15] with a very special challenge for ecofriendly bio-based plastics.[16,17] The development strategy of engineered nano-materials aims also to endow materials with innovative functionalities such as antimicrobial, gas permselectivity, nano-bio-sensing *etc*. These innovative functions partake in the advent of active and intelligent packaging that are able to contribute to the prevention of the waste and losses of perishable products, such as food or other bio-products.[18] For example, polyethylene (PE)/organoclay composites are one of the most studied nano-enabled composite packaging materials because of their improved barrier properties at very low loading levels compared

with conventional filler composite.[19,20] The production of these composite blends have been widely investigated by 3 different approaches; melt blending and processing,[15] liquid dispersion and solution casting[9] and in situ polymerization.[8] Highly exfoliated impermeable MMT platelets make the diffusion length longer by creating a tortuous path, expected to improve the barrier performance of the composite.[21]

One of the main challenges for expressing the unique properties of NPs (such as mechanical, barrier, and fire retardant properties) deals with the achievement of a sufficient exfoliation of NPs in the polymeric matrix. Partially exfoliated and intercalated structure is frequently observed.[22,23] To enhance the dispersion of the particles into a polymer matrix, addition of a compatibilizer and/or chemical modification of the particle surface with the aim to match the polymer matrix polarity, is often carried out.[9,11] For instance, in the case of clay platelets, cationic exchange of the inorganic interlayer cations by organic ones, such as alkylammonium surfactants, is one of the most commonly used techniques. However, the possible level of nano-clay incorporation remains low, generally between 1 and 5 up to 10% wt%.[24] Therefore, it is important to note that such a low maximal NPs loading is due to the difficult dispersion of NPs in a polymer matrix and therefore the advantage of nano reinforcement is de facto auto-limited.[25]

In a composite material, the properties of each constituent can be better expressed when these constituents are structured into multilayered structures rather than homogeneous blends.[21,26–28] In this way, alternating regular polymers and NPs layers enables to design nano-enabled composite layered structures, containing higher NP% and showing innovative properties related to NPs layers. Different processing techniques are used to fabricate multilayer nano-enabled composite, such as spin-coating, thermal deposition, chemical self-assembly *etc*.[29,30] Layer-by-Layer (LbL) self-assembly is one of the most promising techniques that offers to achieve a layered structuring and stands out due its ability to finely control nanomaterial dispersion and interfacial interactions leading to a wide range of applications.[31,32] It can be effectively applied to the coating of planar substrates and curved surfaces regardless of shape and size. The architecture can be designed with nanometer precision to meet different requirements such as thickness, controlled permeability, conductivity, *etc*.[31] LbL multilayer nano-enabled composite show improved properties compared to conventional blends and enable to reveal the proper properties of each layer, especially the NPs barrier properties.[21,26]

Conventional polymers, petro-polymers but also promising bio-polymers that are commonly used as packaging materials, are uncharged polymers and LbL assembly cannot apply without sophisticated strategy such as ultrasonic, plasma and UV/ozone treatment of the substrate,[33,34] which however, do not allow further successive deposition of uncharged substances layers. Therefore alternative technology for multilayer structuration of uncharged constituents is required to produce multilayer nano-enabled composite films using conventional packaging polymers. With the advancement in the LbL technique and the requirement of different properties and functions for multilayer films which are not achievable by the use of charged components, non-electrostatic interactions have gained great attention and deserve important future development to unlock LbL potentialities. In recent years, hydrophobic interaction and hydrogen bond,[35] charge transfer interactions,[36] host–guest interactions[37] and metal–ligand coordination[38] have been successfully investigated for LbL multilayer deposition.

Inspired by the concept of traditional LbL assembly and driven by the lack of similar processes applicable to conventional uncharged and water resistant polymers, which are available for

large applications such as food packaging, the present study aims to demonstrate the feasibility of developing a stratified structure based on uncharged polymer and NPs self-assembly. Such nano-enabled multi-layered structure are expected to open large applications in the area of barrier, active or intelligent multilayers films able to improve food preservation and reduce food and packaging wastes and losses. This study investigates a method of hybrid non-ionic assembling of a system composed of repetitive bilayers of two building blocks: polyethylene and organoclays. PE was selected as one building block because it is one of the most widely used and studied polymers for food packaging,[39] in particular for PE/organoclays nano-composites development to improve its barrier properties.[13,20] Organoclays were selected as a second building block because they were previously demonstrated to be compatible with PE in the development of nano-composites.[40,41] Regarding the good balance of optical and mechanical properties of the PE and the good barrier properties of the organoclay (OMMT) already widely demonstrated in literature, widespread potential applications can be anticipated for the targeted multilayer film such as in agricultural and packaging films, automobile manufacturing, and construction.[13,20] In this study, the assembly and film architecture was investigated with required technics, *i.e.* using profilometry to investigate the repeatability and regularity of layer growth, scanning electron microscopy to confirm layer growth and deepen layers' and interface structure knowledge and contact angle (surface properties) measurements to prove the nature of each layer material.

Experimental

Materials

Linear low density polyethylene pellets (LLDPE, LL 1002YB, density 0.918 g·cm^{-3}, melt flow index (MFI), 2.0 g/10 min at 190°C and 2.16 kg) were supplied by Exxon Mobil Chemical. Organoclay (Cloisite®20A – a natural montmorillonite modified with dimethyl-ditallow quaternary ammonium salt with a CEC of 95 meq./100 g clay mineral and a basal distance value d_{001} = 2.65 nm) was purchased from BYK additives & instruments (density: 1.77 g·cm^{-3}, moisture: <3%, typical dry particle size: <10 µm (d_{50})). Single-side-polished (100) silicon wafers (Si-Mat Silicon Materials, Germany) with a thickness of 0.5 mm were cleaved and cut in 60 mm × 20 mm rectangular pieces and used as substrate for film growth characterized by profilometry. Toluene (SIGMA-ALDRICH, USA) with a purity ≥ 99.7% was used as solvent. All other chemicals are analytical grade and used as received.

Substrate film preparation

LLPDE substrate films were prepared by extrusion using a corotating twin screw extruder (Thermo Scientific™ EuroLab 16) with a L/D ratio of 40 and a screw diameter of 16 mm, at a screw speed of 200 rpm and a feeding rate of 1.0 kg·h^{-1}. The temperature profile of the extruder from feeder to the die was 160, 165, 165, 170, 170, 175, 175, 180 and 180 °C. The extruder was equipped with a plate die and was connected to calendaring system leading to films 160 µm thick and 10 mm wide.

Multilayer build-up

A LLDPE solution (2%; w/v) was prepared by dissolving 2 g of LLDPE pellets (previously ground) in 100 mL of toluene at 120 °C for 3 hours under stirring.[42] The temperature of the solution was then decreased to 80 °C prior to the layer deposition. Organoclay powder was also dispersed in toluene (2%; w/v) at ambient temperature for 60 minutes under stirring. The

solubility of both solutions was checked through visual and/or microscopic (clear solutions with no visible non solubilized particles) observation of the solutions.
For deposition onto LLDPE substrates, the pieces of film (100 mm × 20 mm) were rinsed with deionized water, methanol and again with deionized water before thorough hot air drying. For deposition onto silicon wafers, all the substrates were cleaned before layers deposition by immersing firstly in a mixed solution of methanol and hydrochloric acid (1 : 1, v/v) for 30 min and then stored in a concentrated sulfuric acid solution for at least 12 hours. All the wafers were then extensively rinsed using Milli-Q water and used within a few hours for the deposition of multilayer films.
Each substrate was then dipped in the organoclay dispersion for 2 s, taken out, thoroughly rinsed with toluene, and dried with hot air. The same procedure was then applied using the LLDPE solution instead of the organoclay dispersion. After this initial bilayer was deposited, the same deposition procedure was repeated until reaching the desired number of bilayers. A scheme of the self-assembly deposition technique and 3D cross sectional illustration of the resulting multilayer nanostructure are shown in Fig. 1.

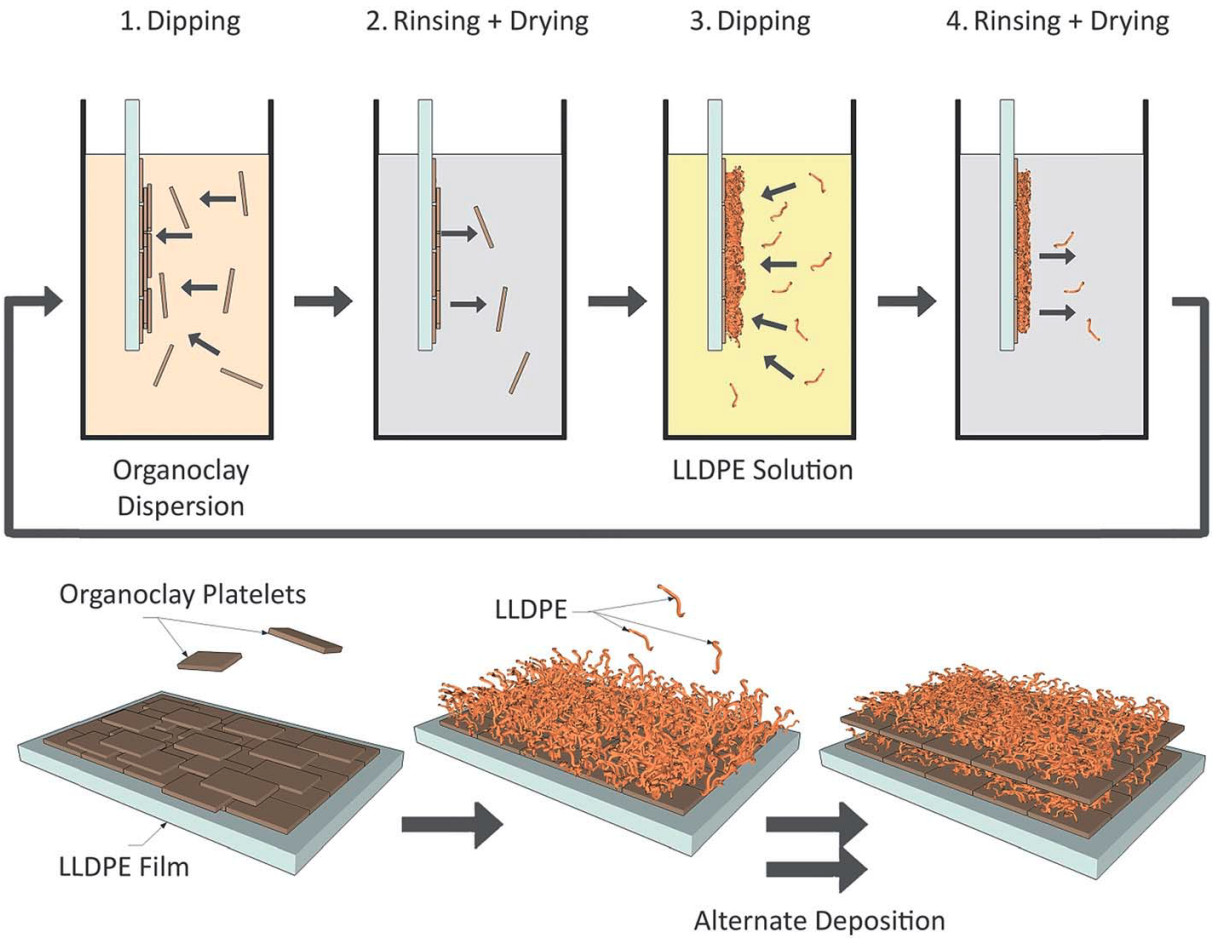

Fig. 1. *Schematic of the Self-assembly deposition technique and 3D cross sectional illustration of the resulting multilayer nanostructure.*

Material characterization

After each layer deposition, the multilayer growth was monitored using a stylus profilometer (Veeco Dektak 150). The film thickness was deduced from the step formed between the layer and the uncovered substrate. The morphology of the multilayer surface and cross-section was

examined using a scanning electron microscope (SEM S-4500, Hitachi, Japan) at an accelerating voltage of 2 kV. Samples were cryo-fractured under liquid nitrogen before being mounted and gold/palladium coated by ion sputtering. The surface properties of the multilayer films were investigated by the sessile drop method using a goniometer equipped with a CCD camera (25 frames per s) (Digidrop, GBX, France). The contact angle measurements were made at equilibrium after deposition of a 3 µL pure water droplet at the surface of each film. Measurements were performed in duplicate on three different areas of each sample at room temperature and relative humidity.

Results & discussion

Building blocks and layer deposition process

A novel multilayer self-assembly driven by non-ionic interactions at liquid–solid interfaces was investigated. The multilayer build-up started here from an uncharged polymer substrate and consisted in successively depositing uncharged an organoclay layer and uncharged polymer layer with subsequent repeating depositions.

For the successful construction of these self-assembled multilayers, a hypothesis was set up that apolar building blocks should be first solubilized or dispersed in an adequate solvent. Then, in the presence of this solvent, these two initially soluble constituents should be able to form an insoluble structure by setting up multiple intermolecular interactions, leading to the formation of a repetitive layered structure in controlled environmental conditions. As for conventional ionic LbL assembly, which depends on a set of control parameters such as adsorption times and temperatures, rinsing times, pH, concentration,[31,43] the processing conditions of the self-assembly developed in the present study required to be first explored. Considering that hydrophobic interaction between such apolar building blocks is entropy-driven and thus essentially sensitive to environmental conditions such as temperature, pressure and/ or the presence of various molecules,[44] the identification of processing parameters enabling to achieve a stable and homogeneous multilayer structure had to be first investigated, based on the characteristics and properties of each building block. For this purpose, different parameters identified as influential on the multilayer build-up have been explored such as the conditions of dipping bath and rinsing steps (solvent nature, time, temperature) as well as drying step (temperature, time).

The first building block is an organically modified montmorillonite (MMT) nanoclay, so-called “organoclay”. In order to increase the affinity of MMT with the hydrophobic polymer, MMT nanoclays are modified with quaternary alkyl ammonium salts to increase both the basal spacing and the effective interaction (and therefore exfoliation) of layered silicate with the surrounding apolar media such as a melted hydrocarbon polymer.[19,45,46] Hydrophobic dimethyl-bis (hydrogenate tallow) ammonium was reported to be the most suitable MMT modifier to develop PE based nanocomposites.[19,47,48] For the production of the organoclay used in this study, the hydrogenated tallow added during the organic modification was derived from a natural product with a carbon average of 17 (Cloisite 20A). The selected organoclay is one of the most hydrophobic organically modified MMT clays, with densely organized alkyl chains and a surface energy similar to paraffin.[49] Organoclay powder was dispersed at 20 °C in toluene solvent to obtain a transparent dispersion. Toluene is a dispersive solvent that is expected to develop interactions with the tallow's alkyl group and insert between the intergallery regions leading to more efficiently swelling the intercalated organic chains. It was reported to be the best solvent used for solution intercalation of organoclays

such as the one used in the present study.[49–52] Toluene is also expected to contribute to opening the internal space between the stacked layers and making the organic modifier parts more accessible for interacting with the hydrophobic PE surface. Atfirst, the PE film substrate was dipped at 20 °C in the organoclay dispersion. These initially well-dispersed organoclays were expected to form an insoluble structure with the PE substrate surface by setting up multiple intermolecular interactions with the PE molecules. Then a short rinsing step using toluene at 20 °C instead of water was demonstrated to reduce the variability of the thickness of the organoclay layers by removing uniquely the loosely attached materials. The organoclay–PE aggregation mechanism was hypothesized to be related to a higher affinity of organoclays with PE than with the solvent.

The organoclay-coated film substrate was then dipped in the solution of the second building block, which is PE. PE is a nonpolar, saturated, high molecular weight hydrocarbon, with a relatively straight polymer chain on which short side chains can be branched.[53] The polyethylene (LLDPE) used in this study is a substantially linear polymer displaying numerous short branchings, made by copolymerizing ethylene with a short chain alpha-olefin (1-butene) and has a complete hydrophobic structure. A PE building block is soluble in hydrocarbons or chlorinated hydrocarbons (e.g. toluene, xylene, trichloroethylene) above its melting temperature54 and remains soluble at temperatures equal or above 80 °C. PE materials were solubilized using toluene at 120 °C. The same solvent was chosen on purpose for both building blocks in order to avoid the problem of cross-contamination of the following deposition solution by solvent adhering on the surface of, or residual solvent inside, the previous layer as observed in LbL assembly.[31] During the deposition step of the PE layer, special attention had to be paid to keep the integrity of the PE film substrate and subsequent deposited PE layers by limiting the temperature of the solvent and the duration of the dipping step. The dipping temperature had to be decreased to 80 °C and the dipping time limited to 2 s in order to avoid PE swelling by solvent absorption leading to further substrate bending or PE substance being desorbed leading to an inhomogeneous or even discontinuous PE layer. After dipping in the PE solution, the film was rinsed with toluene at 20 °C and dried with hot air to reduce the initial high variability of the thickness of the PE layer. It is recognized in literature[42,55] and it was fully verified in the present study that solution of PE in toluene is converted into a white gel when the temperature decreased below 60 °C due to interactive entanglements between solubilized PE chains. Considering that the organoclay-coated film substrate is at 20 °C when dipped in the 80 °C PE–toluene solution, a superficial PE–toluene gel is likely to be formed at the surface of the dipped film, leading to the physical adhesion of a micro-layer of gelified PE solution. The rinsing step here helped the cooling of the deposited PE layer while eliminating the weakly attached PE chains. The drying step enabled the solvent to evaporate rapidly. These cooling and evaporation steps were necessary to stabilize the PE layer, which in turn, stabilized the organoclay layer, which is therefore sandwiched between the polymer layer and the film substrate. This procedure was repeated subsequently to achieve the desired number of layers.

Film growth and layer surface property

The most explicit property of an individual layer is its thickness, which is mostly dependent on the deposition conditions and the nature of the underlying surface.[31] The thickness of the deposited layers versus the number of deposition cycles was measured by profilometry and the growth profile of the multilayer structure is shown in Fig. 2. Samples with an even number of layers exhibited PE building block as the outermost layer, whereas samples with an odd

number of layers exhibited organoclay building blocks as the outermost layer, except the neat PE substrate numbered as layer zero.

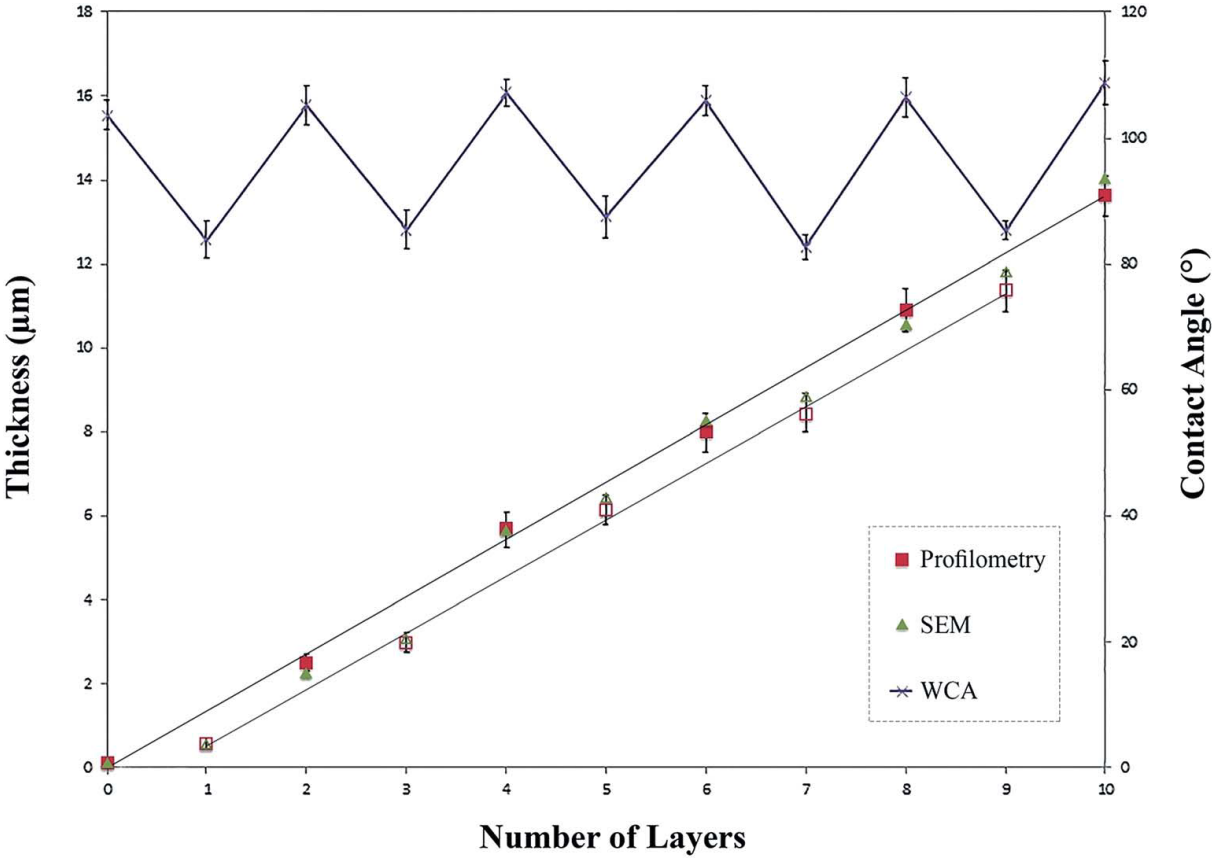

Fig. 2. *Thickness of the deposited layers (profilometry and SEM measurements) and water contact angles on the surfaces of LLDPE substrate film and organoclay/LLDPE multilayer films with different layer numbers. The solid shapes present layers exhibited PE building block as the outermost layer, whereas hollow shapes present layers exhibited organoclay building blocks as the outermost layer. The error bars show the standard deviation.*

The measured film thickness for deposited layers increased linearly with the number of deposition cycles. The thickness growth profile of LbL multi-layer films typically proceeds either linearly or exponentially.[56,57] The linearly and exponentially growing LbL films display rather specific different structure and properties.[32] Film growth increases linearly based on the attractive intermolecular interactions occurring between the dispersed building block and the exposed deposition surface. The layer's growth occurs until the possible intermolecular interactions of the exposed surface are saturated, resulting in a stratified internal structure.[58] Exponentially growing films have a homogeneous internal structure that results from the diffusion of dispersed building blocks into the multilayer film, after having interacted with the exposed surface.[59] In the present study, the film is likely to be highly stratified based on the linear growth pattern exhibited in Fig. 2. Such a linear grown film suggests that none of the two building blocks are able to diffuse significantly throughout the film. The high steric hindrance of the organoclay building block (the unit thickness is ~1 nm, while the lateral dimensions of the clay platelets are from ~100 nm to ~1000 nm up to 2 mm),[60,61] is expected to prevent Fickian's diffusion in the PE layers. Indeed, Šimon *et al.* (2008) predicted that any significant diffusion of nanoparticles in low dynamic viscosity polyolefine such as PE can be expected only in the case of very small iso-dimensional nanoparticles (sphere with a radius in

the order of 1 nm) and without interaction between the polymer and the nanoparticles.[62] PE is the most potentially mobile molecular species able to diffuse, reptate or interdigitate into the bulk. It has been previously demonstrated that MMT clays, despite their well-known barrier function, do not prevent exponential growth of LbL films due to a fast diffusion and/or reptation of polymer such as PEI/PAA in layered structures.[63] On the contrary, the linear growth behavior obtained in the present study demonstrated that PE molecules are not able to significantly diffuse into the film. The impermeability of the deposited organoclay layers to PE molecules could be related to their sufficiently stacked organization that would be efficient to prevent the diffusion of PE molecules between the clays, and/or an immobilizing effect of PE chains due to PE–organoclay interactions and/or to the rapid gelation of the PE layers.

Further information regarding the structural arrangement of the multilayer film was provided by water contact angle values of each building block layer as also shown in Fig. 2. The repetitive high water contact angles (WCA) values (105.1–108.8°) obtained for the even number layers and the substrate PE layer number 0 (105°) are consistent with the high WCA value expected for PE as reported in previous studies.64,65 It confirms the nature and the surface integrity of each deposited PE layer. It could be noted that the small increasing trend of WCA observed for the PE layers when compared to the PE substrate (layer 0) could be related to either a slight modification of the crystallinity of PE caused by its dissolution as previously reported66 or more likely, to an increase in surface roughness as discussed below. Odd number layers clearly exhibited repetitive lower water contact angles (82.6–87.5°) than PE (Fig. 2) therefore confirming the different surface properties of the organoclay layers. These WCA values are in between the average values of 95° ± 2° and 67° ± 3°, previously reported for the same organoclays of static advancing contact angle measured on compacted powder clays and on vibration-induced equilibrium contact angle respectively.[67] Indeed the measurement of the surface properties of clay powder is a difficult task due to liquid absorption during the experiments but also interfacial tension or surface roughness.[67,68] The measurement obtained in the present study suggested that WCA of a continuous layer of Cloisite 20A, although not an ideal surface, is in the large range of values previously measured on powder using different techniques. The alternate variation of contact angle confirmed the profilometry results, *i.e.* the successful stratified assembly of no-charged organoclays and PE building blocks into multilayer films starting from a simple PE substrate.

Film morphology

The morphology (surface and cross-sectional) of multilayer films is a very important characteristic as it ultimately determines many properties of the materials.[69,70] Fig. 3 and 4 show a selection of electron scanning micrographs of the outer surfaces and cross-sections of the multilayers, respectively.

Significant differences can be observed comparing the neat surface of the PE substrate and the surface of the multilayer films. As can be seen in Fig. 3, the surfaces of the multilayer films are much less smooth and homogeneous than the PE substrate, although they represent a continuous matrix without any pores or cracks suggesting a good structural integrity. The incorporation of organoclay nanoparticles is likely to be the cause of such a surface morphology comprising closely spaced micron- and submicron-sized protrusions. It was previously predicted that a better layer separation can be attained through incorporation of the nanoparticles into multi-layered films, but then a higher film roughness is also expected.[71] While increasing the number of deposited bilayers, the surface of the multilayered coating exhibited an increasingly pronounced roughness with higher irregularities confirming the

multilayer formation and growth by the novel self-assembly technique. The structure and surface roughness of self-assembled multilayer films depends a lot on their underlying surface.[31] Similar results were reported by Pinheiro *et al.*[72] on LbL films made by depositing k-carrageenan and chitosan layers on aminolyzed/charged PET. Similar increases in surface roughness and special surface morphology were also reported by Zhang *et al.*[73] who used high temperature to fabricate LLDPE superhydrophobic film. Surface roughness increase could also be responsible for the slight WCA angle increase with the number of deposited layers as evidenced in Fig. 2. Char *et al.* (2008) concluded that while grainy films were formed using dip-assisted assembly, smoother films were formed by spin-assisted deposition. For the rougher morphology of the dip-assisted films, the contact angle increased as the number of layers increased; conversely, it was independent of the film thickness for the more uniform spin-coated films.[74]

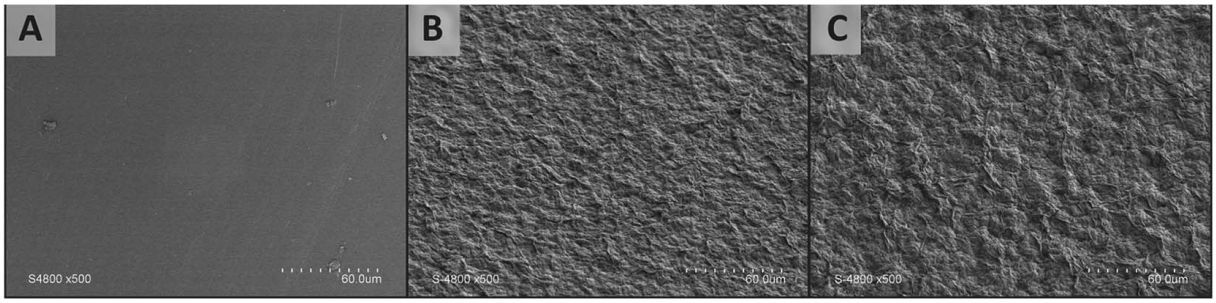

Fig. 3. *Surface morphologies of the multilayers: PE substrate (A), 2× (OMMT/PE) (B), 4× (OMMT/PE) (C).*

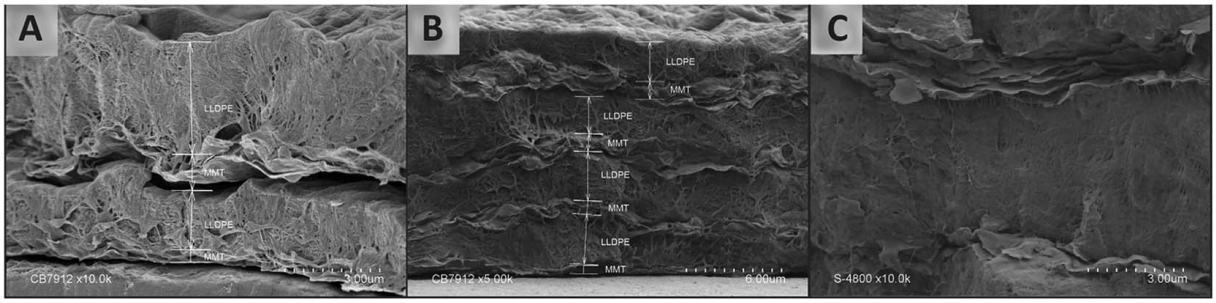

Fig. 4. *Cross section images of the multilayers: 2× (OMMT/PE) (A), 4× (OMMT/PE) (B), OMMT layer (C).*

The formation of the multilayered coating on the PE film surface can be clearly visualized in the cross-section images of the different samples (resembling the schematic images in Fig. 1), corroborating the stratified repetitive structure discussed from profilometric and WCA results. Individual clay platelets can be distinguished between the PE layers at the highest magnification (Fig. 4C). A distinct structure of alternate flaky and compact layers can be seen in the multilayers deposited on the PE film substrate (Fig. 4); the layered structure seems more close-packed for films prepared by depositing more than two bilayers. The presence of occasional, sparsely distributed open voids between two adjacent layers in the cross-section images of one and two bilayers (Fig. 4A) was probably caused by a retraction phenomenon occurring during the film cryofracture prior to the SEM analysis. This might be related to more cohesive structures due to stronger interactions for multilayers made with a higher number of bilayers, as frequently observed in LbL assembly.[32,75,76] Thus, the densely packed structures seen in the images of more than two layers suggested a good adhesion between the PE and organoclay. At high magnification, some cross-connecting strands that can be observed

between the layers (Fig. 4C) might arise as a result of the localized adhesion between the polymer chains of PE and the organoclay layers occurring at the interfaces during the self-assembly process leading to the multilayered structure.

Film layer thicknesses

Through linear regression, the average film growth rate of deposited bilayers is ~2.7 µm per cycle with an approximately 450 nm clay layer and 2.25 µm PE layer forming each bilayer (Fig. 2). The resulting material could be qualified as a "micrometric self-assembled multilayer structure". The two independent thickness measurements deduced from profilometry and SEM cross-section images gave consistent thickness values for each investigated sample (Fig. 2). As already mentioned, the thickness increase is proportional to the nominal number of deposited bilayers, clearly indicating a stable and replicable growth process. The average thickness measured for films made of 10 layers (5 bilayers consecutively deposited) is 13.4 ± 0.3 µm (Fig. 2).

The high PE thickness clearly evidences the formation of a polymer network and therefore the involvement of physical interaction between the surface of the organoclay layer and a sufficient quantity of entangled polymer chains in solution. PE solution is therefore supposed to become highly viscous or even gelified when it comes in contact with the organoclay surface. The temperature decreases of a thin layer of PE solution in contact with the solid surface would be accountable for increasing intermolecular PE interactions to the detriment of interactions with the aromatic ring of toluene.

The thickness of one monolayer of exfoliated organoclays should be about 1 nm.[77,78] The basal spacing related to the hydrocarbon tallow was evaluated to be higher than 2.5 nm in the case of Cloisite 20A,[40,41,79,80] without considering the swelling effect of the solvent. Therefore, individual exfoliated organoclay is expected to display a thickness of about 4 to 5 nm. The organoclay layer thickness measured in the present study suggested that a high number of clay platelets are deposited per cycle. Theoretically, there should be around one hundred stacked individual organoclays in one layer. However the microscopic observation of the organoclay layer (Fig. 4C) revealed that the layer is not an ideally planar deposition of organoclay entities and that their number seems to be much less important than calculated. Although the obtained organoclay-toluene solution was perfectly transparent, a non-exfoliated form of organoclay was previously demonstrated[52] in the same organoclay–toluene solution, at the same temperature and percentage. Organoclay platelets aggregate to make particles of an estimated dimension up to 50 nm. It is likely that the entities visible on the microscopic observation of the organoclay layers are these stacked platelets named tactoids and that a set of about ten of them, far from being perfectly horizontally aligned, constitute the organoclay layer thickness. This observation clearly demonstrated that the organoclay layer was not limited to one monolayer of the organoclay entity (tactoid) present in the solvent and could grow further, which suggested the involvement of a solvophobic-like effect and hydrophobic interactions in the self-assembly mechanism.

It should be noted that, in conventional LbL assembly, a high number of deposition cycles is required to achieve a satisfactory multilayer compact structure (100 nm/ca. 70 deposition cycles) and thickness.[35] Such a tedious and time consuming process leads to efforts for reducing the number of deposition cycles. Strategies like electric field enhanced[81] or pressure enhanced (dynamic deposition)82 procedures have been developed to increase the thickness and compactness of deposited layers, in order to reduce the deposition cycles to less than 10. In the present study, the spontaneous formation of thicker layers of both organoclay and PE

with a linear growth of bilayer thickness remarkably reduced the required deposition cycles without introducing any external forces, thus greatly simplifying the multilayer film fabrication procedure.

Self-assembly process and underlying mechanisms

PE is a highly hydrophobic hydrocarbon chain, which is not electrostatically charged. An organoclay platelet is likely to be charged on the edge of the platelet, while highly hydrophobic hydrocarbon chains occupy its surface. Organoclay and PE do not have any functional groups exerting attractive interactions with each other.[83,84] As a consequence, it was assumed that the self-assembly of organoclays on PE surfaces was driven by solvophobic molecular construction involving hydrophobic interactions between the organic parts of the organoclay tactoids dispersed in an organic solvent and the PE hydrophobic surface (Fig. 5). The hydrophobic association of apolar molecules in aqueous solution demonstrates the intrinsic role that a solvent can play in driving self-assembly processes.[85–87] The general manifestation of this phenomenon in other solvents is called the solvophobic effect.[88] Minimizing the exposure of apolar surface to the solvent more generally arises from the change of the balance between solvent–solute interactions and cohesive solute-solute interactions, in favour of these last interactions.[89] When applied to liquid chromatography (LC), solvophobic theory apprehends the retention of solutes on the stationary phase partly to the rejection of solute molecules by the solvent, and partly to the attraction of the solute molecules by the stationary phase.[90] Even though the concept of solvophobic effect is mostly studied for apolar solutes in aqueous media, an analogous effect was demonstrated to take place in organic solvents.[91-93] Recently, Sedov *et al.*[94] evidenced that the solvophobic effect was indeed related to the self-association of solvent molecules without necessarily the presence of solvent-solvent hydrogen bonds. Akashi *et al.*[95] reported an solvophobic effect to explain the building up of a LbL layered structure made of poly(vinyl alcohol) (PVA) and poly(methyl methacrylate) (PMMA). Linear apolar hydrocarbon molecules with the greatest number of carbons are known to make the strongest and most dense interaction zones,[96] the culminating state of strength and density being the crystallized areas. The significant role played by the hydrophobic interactions in the traditional LbL assembly was highlighted by Kotov.[97] He showed several examples of multilayers building up in which strong electrostatic attraction of opposite charges located on a substrate and on a substance to be assembled did not guarantee the formation of multilayers and reported that driving forces such as hydrophobic interactions have to be considered as the layer-by-layer adsorption forces for the preparation of LbL films of proteins, alumosilicates, dyes, polymers and nanoparticles. Later, other research showed the possibility to use hydrophobic interactions along hydrogen bonds as the main forces for successful LbL assembly instead of the traditional ionic ones.[35] To the best of our knowledge, the closest study to the present one was conducted by Sabapathy *et al.*[98] who evidenced hydrophobic attractive interactions as the only driven force for the synthesis of patchy particles through a simple dip coating method. They formed a silica particle monolayer with polymer patches on the surfaces of the particles and revealed that the hydrophobic interaction between patch–patch regions of single and multipatch particles lead to the formations of finite sized clusters.

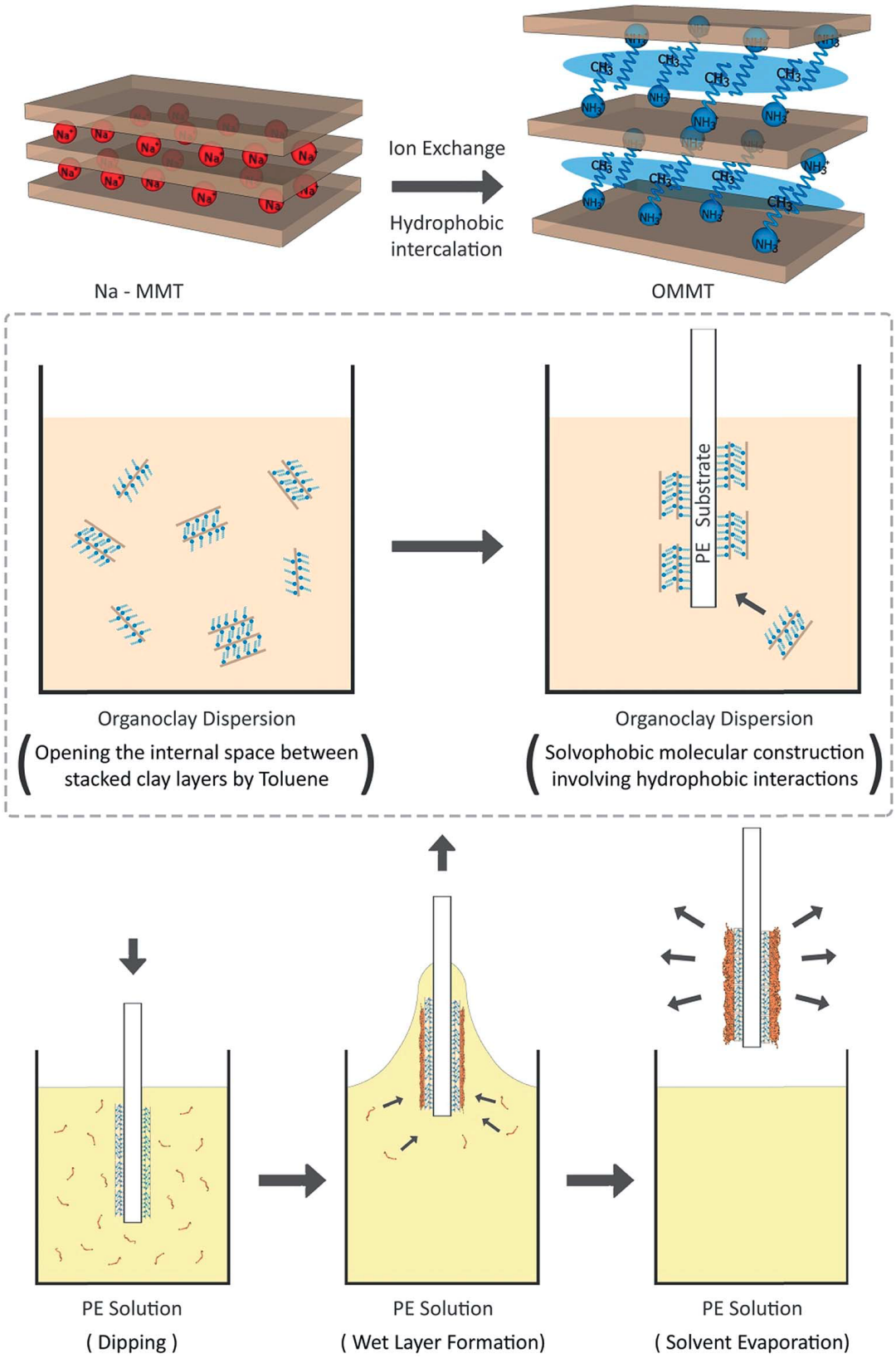

Fig. 5. *Schematic of the self-assembly process and underlying mechanisms.*

In the present study, the self-assembly of PE molecules on organoclay layers is assumed to be the result of a dip-coating process involving physical sorption of a highly viscous PE solution on the surface of organoclay layers (Fig. 5). Such dipcoating method was performed by Contreras *et al.*[99] who successfully fabricated superhydrophobic nanocomposite coatings on

injection-molded polypropylene (PP) films, by dipping the PP samples for a few seconds in hot xylene solutions containing functionalized titanium dioxide nanoparticles and dissolved PP. Taking into account the contact angles results obtained in the present study, showing that the organoclay layer was less hydrophobic than the PE one, it appeared unlikely that the solvophobic effect could be the driving force between the PE molecules solubilized in toluene and the organoclay layer.

Conclusion

A novel methodology for multilayer self-assembly was developed on the basis of the solvophobic effect and further physical adsorption and used to fabricate organoclay/PE multilayer nano-enabled composite films. Based on profilometry, WCA and SEM imaging results, the successful preparation of the self-assembled multilayer on PE film substrate was demonstrated for the first time with a well-defined stratified structure with alternate repetitive layers and without any PE surface pretreatment. This stratified structure with successive thin compact layers is difficult to achieve by other fabrication technologies. Microscale layer growth is achievable and evidenced by a linear film growth rate per deposition cycle measured on the cross-sectional surfaces under SEM and by profilometry. MMT nanoclay platelets with layered inorganic solid structures and a high aspect ratio are expected to enable the development of innovative barrier materials, potentially applicable to the high environmentally impacting area of food packaging. For example low environmental impact multi-layered packaging materials are intended to be developed relying on (i) the high oxygen barrier properties of organoclays, which provides food protection from spoilage and increase its shelf-life and on (ii) the use of eco-friendly polymers such as bio-sourced PE or by substituting PE with bio-sourced and biodegradable polyesters. Now that the feasibility of such novel stratified nano-enabled composite has been demonstrated, further investigation is needed to study the relationship between the functional properties and the structure of these materials, for example by varying the thickness and process conditions and simultaneously evaluating targeted functional properties.

References

1) Z. W. Peter, C. LeBaron and T. J. Pinnavaia, *Appl. Clay Sci.*, 1999, **15**, 11–29.
2) P. G. Chandramika Bora, S. Baglari and S. K. Dolui, *J. Appl. Polym. Sci.*, 2013, **129**, 3432–3438.
3) M. S. Lakshmi, B. Narmadha and B. S. R. Reddy, *Polym. Degrad. Stab.*, 2008, *93*, 201–213.
4) N. Grossiord, J. Loos, L. van Laake, M. Maugey, C. Zakri, C. E. Koning and A. J. Hart, *Adv. Funct. Mater.*, 2008, **18**, 3226–3234.
5) Y. Shi, T. Kashiwagi, R. N. Walters, J. W. Gilman, R. E. Lyon and D. Y. Sogah, *Polymer*, 2009, **50**, 3478–3487.
6) A. Kalendova, D. Merinska, J. F. Gerard and M. Slouf, *Polym. Compos.*, 2013, **34**, 1418–1424.
7) Q. Chaudhry, M. Scotter, J. Blackburn, B. Ross, A. Boxall, L. Castle, R. Aitken and R. Watkins, *Food Addit. Contam., Part A: Chem., Anal., Control, Exposure Risk Assess.*, 2008, **25**, 241–258.
8) F. Chivrac, E. Pollet and L. Avérous, *Mater. Sci. Eng.*, R, 2009, **67**, 1–17.
9) O. Faruk, A. K. Bledzki, H.-P. Fink and M. Sain, *Prog. Polym. Sci.*, 2012, **37**, 1552–1596.
10) S. Sinha Ray and M. Okamoto, *Prog. Polym. Sci.*, 2003, **28**, 1539–1641.
11) S. Ray, S. Y. Quek, A. Easteal and X. D. Chen, *Int. J. Food Eng.*, 2006, **2**, 5.
12) T.-S. Chung, L. Y. Jiang, Y. Li and S. Kulprathipanja, *Prog. Polym. Sci.*, 2007, **32**, 483–507.
13) H. Cong, M. Radosz, B. Towler and Y. Shen, *Sep. Purif. Technol.*, 2007, **55**, 281–291.

14) S. Pavlidou and C. D. Papaspyrides, *Prog. Polym. Sci.*, 2008, **33**, 1119–1198.
15) V. Mittal, *J. Appl. Polym. Sci.*, 2008, **107**, 1350–1361.
16) M. Martínez-Sanz, A. A. Vicente, N. Gontard, A. Lopez-Rubio and J. M. Lagaron, *Cellulose*, 2014, **22**, 535–551.
17) T. Cagnon, C. Guillaume, V. Guillard and N. Gontard, *Packag. Technol. Sci.*, 2013, **26**, 137–148.
18) N. Bumbudsanpharoke and S. Ko, *J. Food Sci.*, 2015, **80**, R910–R923.
19) L. B. de Paiva, A. R. Morales and F. R. Valenzuela Díaz, *Appl. Clay Sci.*, 2008, **42**, 8–24.
20) S. Sánchez-Valdes, M. L. López-Quintanilla, E. Ramírez- Vargas, F. J. Medellín-Rodríguez and J. M. Gutierrez-Rodriguez, *Macromol. Mater. Eng.*, 2006, **291**, 128–136.
21) M. A. Priolo, D. Gamboa and J. C. Grunlan, *ACS Appl. Mater. Interfaces*, 2010, **2**, 312–320.
22) P. Mederic, L. LE Pluart, T. Aubry and P.-J. Madec, *J. Appl. Polym. Sci.*,2013, **127**, 879–887.
23) K. Stoeffler, P. G. Lafleur and J. Denault, *Polym. Eng. Sci.*, 2008, **48**, 2459–2473.
24) C. Wolf, PhD Thesis, University of Montpellier, 2014.
25) J. Jancar, J. F. Douglas, F. W. Starr, S. K. Kumar, P. Cassagnau, A. J. Lesser, S. S. Sternstein and M. J. Buehler, *Polymer*, 2010, **51**, 3321–3343.
26) S. L. Schirmer, *An Investigation of Multilayer Nanocomposite Polypropylene Film for Food Packaging Applications*, University of Massachusetts Lowell, Massachusetts, 2007.
27) Y. Li, X. Chen, Q. Li, K. Song, S. Wang, K. Zhang, Y. Fu, Y. H. Jiao, T. Sun, F. C. Liu and E. H. Han, *Langmuir*, 2014, **30**, 548–553.
28) C. H. Gu, J. J. Wang, Y. Yu, H. Sun, N. Shuai and B. Wei, *Carbohydr. Polym.*, 2013, **92**, 1579–1585.
29) A. Hambardzumyan, M. Molinari, N. Dumelie, L. Foulon, A. Habrant, B. Chabbert and V. Aguie-Beghin, *C. R. Biol.*, 2011, **334**, 839–850.
30) A. D. Zamkovets, *J. Opt. Technol.*, 2014, **81**, 361.
31) J. B. S. G. Decher, *in Multilayer Thin Films: Sequential Assembly of Nanocomposite Materials*, Wiley-VCH Verlag GmbH & Co. KGaA, 2nd edn, 2012.
32) M. Michel, V. Toniazzo, D. Ruch and V. Ball, *ISRN Mater. Sci.*, 2012, **2012**, 701695.
33) M. Jokar, R. A. Rahman and L. C. Abdullah, *J. Nano Res.*, 2014, **27**, 53–64.
34) S. Azlin-Hasim, M. C. Cruz-Romero, E. Cummins, J. P. Kerry and M. A. Morris, *J. Colloid Interface Sci.*, 2016, **461**, 239–248.
35) J. Zhao, F. Pan, P. Li, C. Zhao, Z. Jiang, P. Zhang and X. Cao, *ACS Appl. Mater. Interfaces*, 2013, **5**, 13275–13283.
36) R. N. Y. Shimazaki, S. Ito and M. Yamamoto, *Langmuir*, 2001, **17**, 953–956.
37) A. Van der Heyden, M. Wilczewski, P. Labbe and R. Auzely, *Chem. Commun.*, 2006, 3220–3222.
38) X. Wang, Z. Jiang, J. Shi, Y. Liang, C. Zhang and H. Wu, *ACS Appl. Mater. Interfaces*, 2012, **4**, 3476–3483.
39) M. R. M. A. N. V. Varadharaju, Indian *J. Eng. Mater. Sci.*, 2012, **19**, 54–66.
40) R. B. E. M. Araújo, A. D. Oliveira, C. R. S. Morais, T. J. A. deMélo and A. G. Souza, *J. Therm. Anal. Calorim.*, 2007, **87**, 811–814.
41) M. Z. F. Tanasa, *Chem. J. Mold.*, 2014, **9**, 106–111.
42) N. N. S. L. Wong and T. A. T. Abdullah, Presented in part at the 4th International Graduate Conference on Engineering Science & Humanity, Johor, 2013.
43) A. Shafir and D. Andelman, *Eur. Phys. J. E: Soft Matter Biol. Phys.*, 2006, **19**, 155–162.
44) B. Widom, P. Bhimalapuram and K. Koga, *Phys. Chem. Chem. Phys.*, 2003, **5**, 3085.
45) P. J. Bardziński, *Appl. Clay Sci.*, 2014, **95**, 323–339.

46) M. Huskić and M. Zigon, *J. Appl. Polym. Sci.*, 2009, **113**, 1182–1187.
47) S. Hotta and D. R. Paul, *Polymer*, 2004, **45**, 7639–7654.
48) R. K. Shah and D. R. Paul, *Polymer*, 2006, **47**, 4075–4084.
49) D. Burgentzle, J. Duchet, J. F. Gerard, A. Jupin and B. Fillon, *J. Colloid Interface Sci.*, 2004, **278**, 26–39.
50) Y. S. Bhole, S. D. Wanjale, U. K. Kharul and J. P. Jog, *J. Membr. Sci.*, 2007, **306**, 277–286.
51) R. M. B. D. L. Ho and C. J. Glinka, *Chem. Mater.*, 2001, **13**, 1923–1931.
52) C. J. G. D. L. Ho, *Chem. Mater.*, 2003, **15**, 1309–1312.
53) K. S. Whiteley, 2011, DOI: 10.1002/14356007.a21_487.pub2.
54) D. B. Malpass, *Introduction to Industrial Polyethylene: Properties, Catalysts, and Processes*, Wiley, 2010.
55) R. Y. G. M. I. Voronova and A. G. Zakharov, *Fibre Chem.*, 2007, **39**, 388–391.
56) C. B. N. Laugel, M. Winterhalter, J. C. Voegel, P. Schaaf and V. Ball, *J. Phys. Chem. B*, 2006, **110**, 19443–19449.
57) K. L. M. Saloma and J. Kankare, *Anal. Chem.*, 2003, **75**, 5895–5904.
58) V. B. E. Hubsch, B. Senger, G. Decher, J. C. Voegel and P. Schaaf, *Langmuir*, 2004, **20**, 1980–1985.
59) C. Picart, J. Mutterer, L. Richert, Y. Luo, G. D. Prestwich, P. Schaaf, J. C. Voegel and P. Lavalle, *Proc. Natl. Acad. Sci. U. S. A.*, 2002, **99**, 12531–12535.
60) Handbook of Layered Materials, ed. S. M. Auerbach, K. A. Carrado and P. K. Dutta, Marcel Dekker, New York, 2004.
61) W. Powrie, *Soil mechanics: concepts and applications*, Taylor & Francis, 2004.
62) Q. C. P. Šimon and D. Bakoš, *J. Food Nutr. Res.*, 2008, **47**, 105–113.
63) M. M. P. Podsiadlo, J. Lee, E. Verploegen, N. Wong Shi Kam, V. Ball, X. J. Lee, Y. Qi, J. Hart, P. T. Hammond and N. A. Kotov, *Nano Lett.*, 2008, 8, 1762–1770.
64) A. K. A. Gitchaiwat, K. Sombatsompop, B. Prapagdee, K. Isarangkura and N. Sombatsompop, *J. Appl. Polym. Sci.*, 2013, **128**, 371–379.
65) L. Li, J. Yin, G. Costa and P. Stagnaro, *J. Appl. Polym. Sci.*, 2009, **111**, 1268–1277.
66) T. C. C. Feng Fana, *J. Chem. Phys.*, 1995, **103**, 9053–9061.
67) A. Pegoretti, A. Dorigato, M. Brugnara and A. Penati, *Eur. Polym. J.*, 2008, **44**, 1662–1672.
68) G. Malucelli, S. Ronchetti, N. Lak, A. Priola, N. T. Dintcheva and F. P. La Mantia, *Eur. Polym. J.*, 2007, **43**, 328–335.
69) C. C. Buron, C. Filiâtre, F. Membrey, C. Bainier, L. Buisson, D. Charraut and A. Foissy, *Thin Solid Films*, 2009, **517**, 2611–2617.
70) A. A. Motedayen, F. Khodaiyan and E. A. Salehi, *Food Chem.*, 2013, **136**, 1231–1238.
71) V. P. J. Jeon, J. Pan and A. V. Dobrynin, *Langmuir*, 2006, **22**, 4629–4637.
72) A. C. Pinheiro, A. I. Bourbon, B. G. D. S. Medeiros, L. H. M. da Silva, M. C. H. da Silva, M. G. Carneiro-da-Cunha, M. A. Coimbra and A. A. Vicente, *Carbohydr. Polym.*, 2012, **87**, 1081–1090.
73) Z. Yuan, H. Chen, J. Zhang, D. Zhao, Y. Liu, X. Zhou, S. Li, P. Shi, J. Tang and X. Chen, *Sci. Technol. Adv. Mater.*, 2016, **9**, 045007.
74) J. L. L. J. Seo, J. Kim, P. T. Hammond and K. Char, *Langmuir*, 2008, **24**, 7995–8000.
75) S. D. Hujaya, J. F. Engbersen and J. M. Paulusse, *Pharm. Res.*, 2015, **32**, 3066–3086.
76) H. Lee, *Phys. Chem. Chem. Phys.*, 2016, **18**, 6691–6700.
77) V. Mittal, *Materials*, 2009, **2**, 992–1057.
78) H. Chen, G. Zhang, Z. Wei, K. M. Cooke and J. Luo, *J. Mater. Chem.*, 2010, **20**, 4925–4936.
79) T. K. D. Nwabunma, *Polyolefin composites*, John Wiley & Sons, 2008.

80) B. G. Soares, A. A. Silva, A. P. Sollymossy, R. A. Braga and J. Duchet, *Appl. Clay Sci.*, 2013, **83–84**, 244–252.
81) P. Zhang, J. Qian, Q. An, X. Liu, Q. Zhao and H. Jin, *J. Membr. Sci.*, 2009, **328**, 141–147.
82) G. Zhang, N. Wang, X. Song, S. Ji and Z. Liu, *J. Membr. Sci.*, 2009, **338**, 43–50.
83) C. D. H. W. Huang, *Macromolecules*, 2006, **39**, 257–267.
84) W. Huang and C. D. Han, *Polymer*, 2006, **47**, 4400–4410.
85) S. Granick and S. Chul Bae, *Science*, 2008, **322**, 1477–1478.
86) F. Biedermann, W. M. Nau and H. J. Schneider, *Angew. Chem., Int. Ed. Engl.*, 2014, **53**, 11158–11171.
87) C. A. Hunter, *Angew. Chem., Int. Ed. Engl.*, 2004, **43**, 5310–5324.
88) L. Yang, C. Adam and S. L. Cockroft, *J. Am. Chem. Soc.*, 2015, **137**, 10084–10087.
89) E. M. D. Ronis and J. M. Deutch, *Chem. Phys. Lett.*, 1977, **46**, 53–55.
90) S. Ahuja, *Selectivity and detectability optimizations in HPLC*, Wiley, 1989.
91) O. Sinanoglu, *in Molecular Association in Biology*, Academic Press, New York, 1968, p. 427.
92) E. S. J. Penfold, I. Tucker and P. Cummins, *J. Colloid Interface Sci.*, 1997, **185**, 424–431.
93) A. Ray, *Nature*, 1971, **231**, 313–315.
94) I. A. Sedov, M. A. Stolov and B. N. Solomonov, *J. Phys. Org. Chem.*, 2011, **24**, 1088–1094.
95) T. S. M. Akashi, S. Kamimura and N. Kawanishi, *Langmuir*, 2002, *18*, 8381–8385.
96) J. D. P. P. Atkins, *Physical Chemistry for the Life Sciences*, Oxford University Press, Oxford. UK, 2006.
97) N. A. Kotov, *Nanostruct. Mater.*, 1999, **12**, 789–796.
98) M. Sabapathy, S. D. Christdoss Pushpam, M. G. Basavaraj and E. Mani, *Langmuir*, 2015, **31**, 1255–1261.
99) C. B. Contreras, G. Chagas, M. C. Strumia and D. E. Weibel, *Appl. Surf. Sci.*, 2014, **307**, 234–240.